for (hfac)CuL, L = PMe_3, PEt_3 but not for L = 1,5-COD and 2-butyne. These observations indicate that the β-diketonate ligand and Lewis base ligands play a crucial role in determining the deposition selectivity. It is noteworthy that some degree of selectivity has recently been reported (under different conditions) for (hfac)Cu(1,5-COD) below 200 °C for Ta, Cu, Ag, Au, and Cr versus SiO_2 and Si_3N_4.[33]

On the basis of the trends observed for the (β-diketonate)$CuPMe_3$ series, it is tempting to speculate that the cleavage of the β-diketonate ligand is involved in the rate-determining step of the reaction. However, differences in the adsorption/desorption behavior of the reactants and products are likely to be important also and are currently under investigation.[47,48]

Acknowledgment. M.J.H.-S. and T.T.K. thank NSF (No. CHE-9107035) for partially funding this work. M. J.H.-S. thanks the NSF chemical instrumentation program for purchase of a low-field NMR spectrometer, and T.T.K. acknowledges support from the NSF Presidential Young Investigator program (No. CTS-9058538).

Registry No. (hfac)Cu(PMe_3), 135707-05-0; (tfac)Cu(PMe_3), 135707-06-1; (acac)Cu(PMe_3), 135707-07-2; Cu, 7440-50-8; W, 7440-33-7; SiO_2, 7631-86-9; Pt, 7440-06-4.

Synthesis and Electrochemistry of Conductive Copolymeric Porphyrins

Judith R. Fish,† Eugeniusz Kubaszewski,† Alexander Peat,† Tadeusz Malinski,*,† Jozef Kaczor,‡ Piotr Kus,‡ and Leszek Czuchajowski*,‡

Department of Chemistry, Oakland University, Rochester, Michigan 48309-4401, and Department of Chemistry, University of Idaho, Moscow, Idaho 83843

Received November 18, 1991. Revised Manuscript Received April 9, 1992

This work focuses on electrochemical synthesis and characterization of conductive porphyrinic polymeric and copolymeric materials and their application for electrocatalytic oxidation of methanol and hydrazine and reduction of oxygen directly to water. Conductive polymeric and copolymeric films have been obtained by oxidative electropolymerization of several free-base and metalated porphyrins (*N,N'*-bis[5-*p*-phenylene-10,15,20-tris(3-methoxy-4-hydroxyphenyl)porphyrin]-1,10-phenanthroline-4,7-diamide, H_2-(1,10-phen)$(TMHPP)_2$; 5-*p*-(pyrrol-1-yl)phenylene-10,15,20-tris(3-methoxy-4-hydroxyphenyl)porphyrin, H_2(p-pyr)TMHPP; *meso*-tris(3-methoxy-4-hydroxyphenyl)(*p*-aminophenyl)porphyrin, H_2(p-NH_2)TMHPP) and their respective analogues that contain *p*-tolyl substituents (TTPP) instead of 3-methoxy-4-hydroxyphenyl. Metaloporphyrins with zinc(II) and cobalt(II) have been studied. Studies present evidence to show that the copolymeric new materials can have significantly altered electrocatalytic properties. Copolymers of Zn(1,10-phen) $(TMHPP)_2$ and Zn(*p*-NH_2)TTPP show significant enhancement of catalytic process over their constituents. This was especially true for electrocatalytic oxidation of hydrazine and reduction of oxygen directly to water. Electrocatalytic reduction of oxygen directly to water was enhanced for all copolymers studied. The current density (0.8–1.1 mA/cm^2) for methanol (5%) oxidation on polymeric and copolymeric porphyrins is 5–7 times higher than that observed on a platinum electrode.

Introduction

Porphyrins containing diethylamino,[1,2] [2.2]paracyclophanyl,[2-5] or 3-methoxy-4-hydroxyphenyl[6,7] meso substituents form conductive polymeric films that show good catalytic properties for a number of reactions on electrodes. The role played by the quinonoid system of bonds formed in the intermediates was ascribed as a key factor involved in the polymerization process.[3-5,7,8] We have synthesized some new porphyrin free bases and their metalo derivatives which can be electrochemically polymerized and studied their catalytic properties. Structures and abbreviations of the free bases are shown in Figure 1.

One set of new porphyrins contains 1,10-phenanthroline as an azaheteroaromatic meso substituent with 3-methoxy-4-hydroxyphenyl groups as the remaining substituents. The 1,10-phenanthroline is attached to the porphine by carboxamide-*p*-phenylene bridges at the 4 and 7 positions of the phenanthroline. This linkage forms a diporphine species in which the phenanthroline acts as a "spacer" between the two porphyrin rings. A second set of compounds contains a *p*-(pyrrol-1-yl)phenyl and, a third, *p*-aminophenyl, replacing one of the 3-methoxy-4-hydroxyphenyl substituents. These later compounds are monoporphyrinic. Also, an analogue of each compound has been synthesized with *p*-tolyl substituents instead of the 3-methoxy-4-hydroxyphenyls. Eventually, these analogues will allow polymerization in the absence of the quinone producing 3-methoxy-4-hydroxy substituents to be investigated.

This article reports our investigations of conductive film formation both from the new species and from combinations of these newly synthesized components. The cata-

† Oakland University.
‡ University of Idaho.

(1) Malinski, T.; Bennett, J. E. In *Redox Chemistry and Interfacial Behavior of Biological Molecules*; Dryhurst, G., Niki, K., Eds.; Plenum Press: New York, 1988; p 87.
(2) Bennett, J. E.; Malinski, T. *Chem. Mater.* **1991**, *3*, 490.
(3) Bennett, J. E.; Wheeler, D. E.; Czuchajowski, L.; Malinski, T. *J. Chem. Soc., Chem. Commun.* **1989**, 723.
(4) Czuchajowski, L.; Bennett, J. E.; Goszczynski, S.; Wheeler, D. E.; Wisor, A. K.; Malinski, T. *J. Am. Chem. Soc.* **1989**, *111*, 607.
(5) Czuchajowski, L.; Goszczynski, S.; Wheeler, D. E.; Wisor, A. K.; Malinski, T. *J. Heterocycl. Chem.* **1988**, *25*, 1825.
(6) Malinski, T.; Ciszewski, A.; Fish, J. R.; Czuchajowski, L. *Anal. Chem.* **1990**, *621*, 909.
(7) Malinski, T.; Ciszewski, A.; Bennett, J. E.; Czuchajowski, L. *Proceedings of the Symposium on Nickel Hydroxide Electrodes*; Electrochemical Society: Pennington, NJ, 1990; Vol. 177, p 90.
(8) Malinski, T.; Ciszewski, A.; Bennett, J. E.; Fish, J. R.; Czuchajowski, L. *J. Electrochem. Soc.* **1991**, *138*, 2010.

0897-4756/92/2804-0795$03.00/0

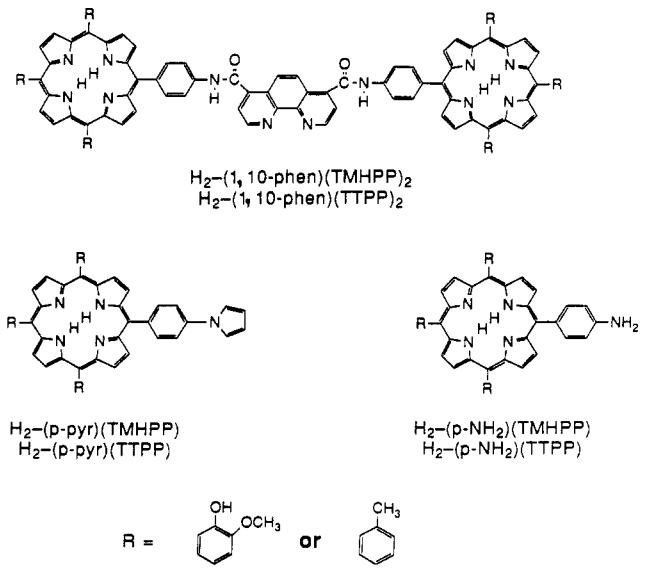

Figure 1. Structure of porphyrin free bases; R = 3-methoxy-4-hydroxyphenyl (TMHPP porphyrins) or R = tolyl (TTPP porphyrins).

lytic properties of the conductive copolymeric porphyrin films are then compared with the properties of each constituent.

Some porphyrinyl derivatives of 1,10-phenanthroline, other than those presented here, have been described in recent literature.[9-12] None, however, was discussed from the point of view of electropolymerization.

The (*p*-aminophenyl)porphyrin is a structural unit in the more complex phenanthroline diporphyrin. Thus, one would expect it to be good reference compound in studies of the electrooxidation/polymerization of the diporphyrin. However, more pertinent to the present work, the *p*-aminophenyl group could promote polymerization via a mechanism characteristic for aniline oxidation.[13,14] The location of 3-methoxy-4-hydroxyphenyl and *p*-aminophenyl in opposite meso positions on the porphyrin can result in the expansion of the quinonoid system of bonds formed during electrooxidation over the whole molecule. Therefore, this compound was also used as a component in copolymerization.

Zinc derivatives were obtained when the synthesis of the free-base systems proceeded more conveniently via these complexes. Catalytic properties of zinc polyporphyrin films have not been investigated previously. As we have found previously that nickel-metalated porphyrins form polymers with very good electrical conductivity and catalytic properties,[6-8] the nickel derivatives were also synthesized and used for copolymerization. The purpose of this work was to see if copolymeric species would be formed and, if so, to survey the catalytic properties of these new materials on methanol and hydrazine oxidation and oxygen reduction. Owing to the significance of these reactions in regard to energy conversion and storage, research on the electrocatalysis of a polymer film electrodes has generally focused on the catalytic oxidation of methanol and hydrazine and on catalytic reduction of dioxygen directly to water. Methanol and hydrazine are considered to be a clean fuel for fuel cells. The cathodic reaction, in fuel cells usually involve reduction of oxygen. Electroreduction of oxygen on metal electrodes proceeds via two, two-electron transfer steps with production of hydrogen peroxide in the first one. Hydrogen peroxide deteriorates the performance of the cathode in fuel cells, but its production can be eliminated by use of catalysts which promote the four electron reduction of oxygen directly to water.

Experimental Section

The new compounds used in the present work are the free-base and/or polymeric porphyrins H_2(1,10-phen)(TMHPP)$_2$ (*N,N'*-bis[5-*p*-phenylene-10,15,20-tris(3-methoxy-4-hydroxyphenyl)-porphyrin]-1,10-phenanthroline-4,7-diamide), H_2(*p*-pyr)TMHPP (5-*p*-(pyrrol-1-yl)phenylene-10,15,20-tris(3-methoxy-4-hydroxyphenyl)porphyrin), H_2(*p*-NH_2)TMHPP (*meso*-tris(3-methoxy-4-hydroxyphenyl)(*p*-aminophenyl)porphyrin) and their respective analogues that contain *p*-tolyl substituents instead of 3-methoxy-4-hydroxyphenyl, H_2(1,10-phen)(TTPP)$_2$ (*N,N'*-bis[5-*p*-phenylene-10,15,20-tris-*p*-tolylporphyrin]-1,10-phenanthroline-4,7-diamide), H_2(*p*-pyr)TTPP (*meso*-tri-*p*-tolyl-*p*-(pyrrol-1-yl)-phenylporphyrin), H_2(*p*-NH_2)TTPP (*meso*-tri-*p*-tolyl(*p*-aminophenyl)porphyrin).

Reagents. 4,7-Dimethyl-1,10-phenanthroline, 2,5-diethoxytetrahydrofuran, vanillin, 4-acetamidobenzaldehyde, thionyl chloride, propionic acid, glacial acetic acid, trifluoroacetic acid, zinc diacetate, nickel diacetate, and the applied solvents (all from Aldrich) were used as received. Pyrrole (99%, Aldrich) was freshly distilled. Selenium oxide was obtained from selenium powder, 99.5% (Aldrich), and concentrated nitric acid. Celite 521 (Aldrich) was used as a filtration agent in the procedure of oxidation with SeO_2. For column chromatography, Florisil 60/200 mesh (Applied Science Laboratories) and silica gel 70–230 mesh (60 Å, Aldrich) were used.

Synthesis. *N,N'*-Bis[5-*p*-phenylene-10,15,20-tris(3-methoxy-4-hydroxyphenyl)porphyrin]-1,10-phenanthroline-4,7-diamide, H_2 (1,10-phen)(TMHPP)$_2$. *General Approach.* This diporphyrin was obtained by condensation of 1,10-phenanthroline-4,7-dicarbonyl chloride with the zinc derivative of *meso*-tris(3-methoxy-4-hydroxyphenyl)(*p*-aminophenyl)-porphyrin, H_2(*p*-NH_2)TMHPP, the latter obtained by deacetylation of the respective *p*-acetaminophenyl derivative. The diacid chloride was obtained by the sequence of the reactions described previously:[12,15] 4,7-dimethyl-1,10-phenanthroline was oxidized by selenium oxide to the dicarboxaldehyde, the latter oxidized by 80% nitric acid to 1,10-phenanthroline-4,7-dicarboxylic acid which finally was converted by thionyl chloride to diacid chloride.

***meso*-Tris(3-methoxy-4-hydroxyphenyl)(*p*-acetamidophenyl)porphyrin and *meso*-Tris(3-methoxy-4-hydroxyphenyl(*p*-aminophenyl)porphyrin, H_2(*p*-NH_2)TMHPP.** Pyrrole (11.1 mL, 0.16 mol) was added to the refluxed mixture of vanillin (18.24 g, 0.12 mol) and 4-acetamidobenzaldehyde (6.52 g, 0.04 mol) in propionic acid (600 mL), and refluxing continued for 3 h. From the mixture left overnight, the propionic acid was distilled off with the addition of small portions of water and then methanol. The residue was dissolved in methylene chloride and chromatographed on Florisil column with 10:1 CH_2Cl_2/MeOH as eluent. The eluate was rechromatographed on the silica gel column with CH_2Cl_2/MeOH 40:1 as an eluent. The middle fraction, evaporated to dryness, gave 2.8 g of raw acetamidophenylporphyrin that was rechromatographed with the same eluent; however, its composition gradually changed from 200:1, 100:1, to 40:1 CH_2Cl_2/MeOH. The pure product (1.71 g) was deacylated by dissolving in trifluoroacetic acid (158 mL) and dropping in concentrated hydrochloric acid (169 mL) at 80 °C. After 20 h, the mixture was extracted with methylene chloride until decoloration of the water phase. The extracts were washed with water and then 10% solution sodium carbonate. The

(9) (a) Gregg, B. A.; Fox, M. A.; Bard, A. J. *Tetrahedron* **1989**, *45*, 707. (b) Salmon, L.; Verlhac, J.-B.; Bied-Charreton, C.; Verchere-Beaur, C.; Gaudemer, G. *Tetrahedron Lett.* **1990**, *31*, 519.

(10) Noblat, S.; Dietrich-Buchecker, C. O.; Sauvage, J. P. *Tetrahedron Lett.* **1987**, *28*, 5829.

(11) Chardon-Noblat, S.; Sauvage, J. P.; Mathis, P. *Angew. Chem.* **1989**, *101*, 631.

(12) Kus, P.; Knerr, G.; Czuchajowski, L. *J. Heterocycl. Chem.* **1991**, *28*, 1.

(13) Ohsaka, T.; Ohnuki, Y.; Oyama, N.; Katagiri, G.; Kamisako, K. *Electroanal. Chem.* **1984**, *161*, 399.

(14) Huang, W. S.; Humphrey, B. D.; MacDiarmid, A. G. *J. Chem. Soc., Faraday Trans. 1* **1985**, *82*, 2385.

(15) Kus, P.; Knerr, G.; Czuchajowski, L. *J. Heterocycl. Chem.* **1990**, *27*, 1161.

chromatography on the silica gel column, 20:1 $CHCl_3$/MeOH as eluent, yielded 0.9 g of pure H_2(*p*-NH_2)TMHPP. FAB MS (*M* + 1) +767; UV–vis (chloroform, nm) 651, 594, 558, 424 (s); ^{1}H NMR (300 MHz, chloroform) 8.90 (m, 8 H, β-pyrrole), 7.71 (m, 9 H, Ar), 7.28 (m, 4 H, Ar, C_6H_4), 5.95 (br s, 3 H, OH), 3.98 (s, 9 H, CH_3), 3.75 (s, 2 H, NH_2), −2.77 (s, 2 H, NH porphyrin). The free-base porphyrin was then metalated with zinc by boiling its chloroform solution (0.4 g of porphyrin in 100 mL of $CHCl_3$ with saturated methanol solution of zinc diacetate. The completion of metallation was confirmed by the UV–vis spectrum (chloroform): 600, 557, 426 (S). Chromatography purification was not necessary.

Condensation with Phenanthroline Diacid Chloride. In this essential step, the freshly prepared 1,10-phenanthroline-4,7-dicarbonyl chloride was added to the Zn(*p*-NH_2)(TMHPP) (0.15 g) dissolved in methylene chloride (100 mL) and stirring was continued at room temperature for 20 h. TLC (silica gel, 10:1) showed the presence of the three products. The UV–vis spectrum showed the loss of zinc from the porphyrin centers. The column chromatography on silica gel with the $CHCl_3$/MeOH eluent which composition gradually changed from 100:1 to 2:1, resulted in separation of the unreacted free-base porphyrin in the first fraction and the expected H_2(1,10-phen)(TMHPP)$_2$ in the main fraction. UV–vis (methanol, nm) 650, 593, 556, 519, 423 (S); ^{1}H NMR (300 MHz, deuteriochloroform) 8.89 (s, 16 H, β-pyrrole), 8.83 (d, 2 H, phenanthroline, PN, C-2,9), 8.16 (m, 2 H, PN, C-5,6), 7.70 (m, 18 H, Ar), 7.34 (s 8 H, Ar, C_6H_4), 7.30 (m, 2 H, PN, C-3,8), 5.95 (br s, 5 H, OH), 3.98 (s, 18 H, CH_3), −2.79 (s, 4 H, porphyrin). Anal. Calcd for $C_{108}H_{78}N_{12}O_{14}$: C, 73.79; H, 4.42; N, 9.51; O, 12.68%. Found: C, 73.21; H, 4.30; N, 9.67.

The nickel(II) derivative of H_2(1,10-phen)(TMHPP)$_2$ was obtained by refluxing for 4 h the porphyrin (0.177 g, 0.1 mol) dissolved in chloroform (15 mL) with a saturated methanol solution of nickel diacetate (5 mL). The product having the UV–vis spectrum characteristic of a (porphyrinato)nickel: 530.5, 422 (S) (in 10:1 $CHCl_3$/MeOH), was washed with water and evaporated to dryness.

***N,N'*-Bis[5-*p*-phenylene-10,15,20-tri-*p*-tolylporphyrin]-1,10-phenanthroline-4,7-diamide, H_2(1,10-phen)(TTPP)$_2$.** This diporphyrin was prepared as previously described by the authors[12] from *meso*-tri-*p*-tolyl(*p*-aminophenyl)porphyrin, H_2(*p*-NH_2)-(TTPP), and 1,10-phenanthroline-4,7-diacid chloride.

5-*p*-(Pyrrol-1-yl)phenylene-10,15,20-tris(3-methoxy-4-hydroxyphenyl)porphyrin, H_2(*p*-pyr)TMHPP. An advantage was taken of the already known syntheses of N-functionally substituted pyrroles[16] and pyrroloinoles[17] which were properly adapted. H_2(*p*-NH_2)TMHPP (0.22 g, 0.3 mmol) was stirred at room temperature with 0.048 g (0.3 mmol) of 2,5-diethoxytetrahydrofuran dissolved in 50 mL of glacial acetic acid. The progress of the reaction was monitored by TLC (silica gel, $CHCl_3$/MeOH 10:1). After 4 h, acetic acid was removed on the rotavap, the residue treated with chloroform, neutralized with 5% ammonia, washed with water, and dried over sodium sulfate. The first of the four fractions separated on the silica gel column with 5:1 $CHCl_3$/MeOH as eluent (FAB-MS *m/e* (*M* + 1) + values 819 and also a low-intensity signal at 834 *m/e*) appeared corresponding to the expected H_2(*p*-pyr)TMHPP. ^{1}H NMR (300 MHz, deuteriochloroform) 8.89 (m, 8 H, β-pyrrole), 7.90 (m, 4 H, C_6H_4), 7.61 (m, 9 H, H, Ar), 7.18 (m, 2 H, pyrrolyl), 6.85 (m, 2 H, pyrrolyl), 5.95 (br s, 3, OH), 3.98 (s, 9 H, OCH_3), −2.74 (s, 2 H, porphyrin). The fourth fraction of eluate was the unreacted substrate, H_2-(*p*-NH_2)TMHPP. Anal. Calcd for $C_{51}H_{39}N_5O_6$: C, 74.83; H, 4.77; N, 8.56; O, 11.74. Found: C, 74.94; H, 4.91; N, 8.49.

The nickel(II) derivative was obtained by dissolving the first fraction of two pyrrole–porphyrins in DMF and refluxing for 0.5 h with nickel(II) acetate. The mixture was left overnight, the brown precipitate filtered off on the sintered glass filter, washed with chloroform, and chromatographed on the silica gel column with chloroform as the eluent. The first fraction obtained represented now the Ni(*p*-pyr)TMHPP.

***meso*-5-*p*-(Pyrrol-1-yl)phenylene-10,15,20-tri-*p*-tolylporphyrins, H_2(*p*-pyr)TTPP.** Although this is not a new compound (compare ref 18), we could not find the description of its synthesis in the literature. In our approach, the *meso*-tri-*p*-tolyl(*p*-aminophenyl)porphyrin (0.135 g, 0.2 mmol), obtained as previously described by us,[12,15] and glacial acetic acid (5 mL) were mixed with 2,5-diethoxytetrahydrofuran (0.5 mmol) under vigorous stirring, and the temperature was slowly increased until the boiling point was reached. After 1.5 h acetic acid was distilled off on the rotavap and the residue dissolved in chloroform. TLC (silica gel, $CHCl_3$/MeOH) showed disappearance of the substrate and the formation of two more polar products. They were separated by column chromatography on silica gel with chloroform as eluent and then rechromatographed in the same way; yield 17%. FAB MS (*M* + 1) +721; UV–vis (chloroform, nm) 648, 592, 553, 517, 420 (S) (blue-shift of all bands by 1–3 nm as compared to the starting H_2(*p*-NH_2)TTPP); ^{1}H NMR (300 MHz, deuteriochloroform) 8.86 (m, 8 H, β-pyrrole) 8.34 and 7.89 (dd, 9.3 Hz, 4 H, C_6H_4), 8.09 and 7.55 (dd, 8.5 Hz, 12 H, Ar, tolyl), 6.81 (m, 2 H, pyrrolyl), 6.46 (m, 2 H, pyrrolyl), 2.69 (s, 9 H, CH_3), −2.75 (s, 2 H, porph). Anal. Calcd for $C_{51}H_{39}N$: C, 84.83; H, 5.41; N, 9.70. Found: C, 84.78; H, 5.62; N, 9.59.

Metalation with nickel was performed in the same way as metalation of H_2(*p*-pyr)TMHPP: ^{1}H NMR (300 MHz, (deuteriochloroform) 8.74 (m, 8 H, β-pyrrole), 8.20 and 7.82 (dd, 9.3 Hz, 2 H, pyrrolyl), 8.03 and 7.68 (dd, 9 Hz, 4 H, C_6H_4), 7.87 and 7.46 (dd, 8.9 Hz, 12 H, Ar, tolyl), 6.81, 6.46 (m, 2 H, pyrrolyl), 2.62 (s, 9 H, CH_3).

Instrumentation. Mass spectrometry was performed on a fast atom bombardment Micromass 70/70 high-resolution mass spectrometer Model V6 with an 11/250 data system. 3-Nitrobenzyl alcohol was applied as a matrix. NMR spectra were recorded on a Bruker-IBM Af (300 MHz) Fourier transform spectrometer. Electronic absorption spectra of newly synthesized compounds were recorded on a Perkin-Elmer Lambda 4C UV–vis spectrometer, Model C 688–0002.

An IBM Model EC 225 voltammetric analyzer or a Princeton Applied Research Model 273 potentiostat with Model 270 electrochemical analysis system was used for cyclic and differential pulse voltammetry. A Princeton Applied Research Model 173 potentiostat with Model 179 digital coulometer was used for controlled-potential electrolysis (CPE) and coulometry. Bipotentiostat DAE4 Pine Instrument Co. was used for ring-disk voltammetry. All potentials are reported versus aqueous SCE.

UV–visible spectra were obtained with a Tracor Northern optical multichannel analysis system composed of a Tracor Northern 6050 spectrometer containing a crossed Czerny-Turner spectrograph in conjunction with the Tracor Northern 1710 multichannel analyzer. Each spectrum resulted from signal averaging of 100 single, 290–890 nm, 2.5-ms spectral acquisitions simultaneously recorded by a double-array detector with a resolution of 1.2 nm/channel. A four-probe method (Keithley Model 197 Microvolt DMM) was used for conductivity measurements of the films.

Procedures. A glassy carbon or platinum button and a platinum wire served as the working and auxiliary electrodes, respectively, for cyclic and differential pulse voltammetry using a conventional three-electrode configuration. A saturated calomel electrode (SCE), separated from the bulk solution by a fritted glass disk, was used as the reference electrode. The thin layer spectroelectrochemical cell used in spectroelectrochemical studies was built following the design of Lin et al.[19] with a calculated path length of 0.5 mm and platinum mesh as the working electrode.

All films were formed by controlled potential oxidation. Copolymer films were formed by controlled potential oxidation of a 1:1 (moles) mixture of the species involved.

The $Fe(CN)_6^{3-}$/$Fe(CN)_6^{4-}$ couple was used to evaluate electron-exchange properties of these materials in comparison with those of the unmodified glassy carbon and platinum electrodes as well as for the determination of the working area of modified electrodes.

Methodology of Catalysis Studies. Current–potential data for catalysis studies were acquired by cyclic voltammetry. Voltammograms were obtained with an unmodified electrode and

(16) Josey, A. D.; Jenner, E. L. *J. Org. Chem.* **1962**, *27*, 2466.
(17) Raines, S.; Chai, S. Y.; Palopoli, F. P. *J. Org. Chem.* **1971**, *36*, 3992.
(18) Bedioui, F.; Moisy, P.; Bied-Charreton, C.; Devynck, J. *J. Chim. Phys.* **1989**, *86*, 235.
(19) Lin, X. Q.; Kadish, K. M. *Anal. Chem.* **1985**, *57*, 1498.

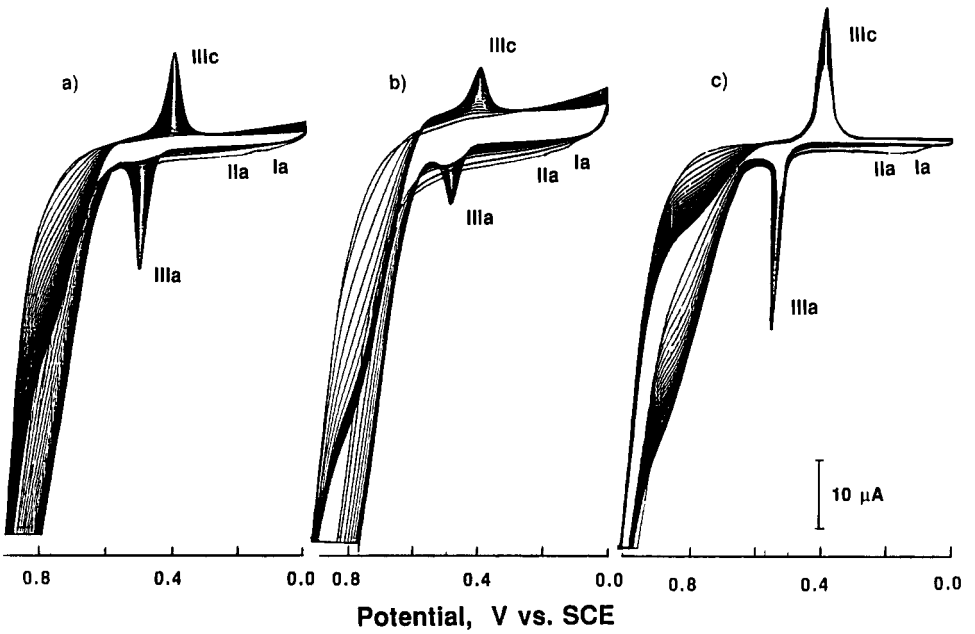

Figure 2. Multiple scan cyclic voltammogram obtained during film formation of Ni(1,10-phen)(TMHPP)$_2$ (a), Ni(*p*-pyr)TMHPP (b), and 1:1 mixture of above two (c) in 0.1 M NaOH; potential scan rate 100 mV s^{-1}.

then with an electrode modified with polyporphyrin in both supporting electrolyte and substrate solution. This ensured that the reaction observed was that of the substrate oxidation rather than a film redox reaction. The catalytic efficiency was evaluated by comparing the peak potential for the film catalyzed process with that of the bare electrode as determined by the difference in peak potential, ΔE_p. Peak currents and current densities were also determined.

Glassy carbon electrodes (area 0.08 cm^2) were used for studies of oxidation of hydrazine as the Pt itself acts as an efficient catalyst for oxidation of this substrate. Platinum button electrodes (0.08 cm^2) were used for the other catalysis studies, e.g., methanol and dioxygen in acidic and basic media. Substrate concentrations were 5% and 10^{-2} M for methanol and hydrazine, respectively. Oxygen concentrations were assumed to be 1.45×10^{-3} M following saturation with oxygen for at least 20 min.

Oxidation of Hydrazine. Voltammograms were obtained using the polymeric film on GCE in 0.1 M NaOH without and with 10^{-2} M hydrazine. Catalytic activity was evaluated by determining the decrease in oxidation potential for the polymer covered versus the bare GCE. As determined previously,[8] the oxidation product was N_2.

Oxidation of Methanol. Voltammograms were obtained using the polymeric film on platinum electrodes in 0.1 M NaOH without and with 5% methanol. The decrease in oxidation potential as well as an increase of current density for the polymer covered versus the bare electode was determined as an indicator of catalytic activity. As with poly-NiTMHPP, the oxidation product was CO_2.[8]

Reduction of Oxygen. Criteria for successful catalytic reduction of dioxygen are a positive shift in E_{pc} and a value of 3.2 mA/[cm^2 (V/s)$^{1/2}$] for the slope of the peak of the four-electron reduction of oxygen.[20] The theoretical value of $i_p/Av^{1/2}$ (where i_p is the peak potential, A the area of electrode, and v the potential scan rate) for a four-electron reduction of O_2 is 3.2 mA/[cm^2 (V/s)$^{1/2}$] for O_2 saturated solution and diffusion coefficient $D_{O_2} = 2.6 \times 10^{-5}$ cm^2 s^{-1}. Voltammograms were obtained using the polymeric film on platinum electrodes first in a deoxygenated and then in a solution saturated with oxygen by bubbling for 20 min. Studies were performed in 1.0 M NaOH, 0.5 M H_2SO_4.

Results and Discussion

Electrochemical Oxidation of Porphyrins in Solution. Anodic peak potentials for the oxidations of the individual compounds investigated by cyclic voltammetry are summarized in Table I. Data, presented previously,[6,8] on H_2TMHPP and NiTMHPP from which the newly synthesized species are derived, are included for comparison. A complicating factor in studying the compounds in this work is that the TTPP species used as control compounds are insoluble in aqueous NaOH, the medium that promotes the desired oxidative polymerization of TMHPP. There are no reductions observed for the TMHPP species in aqueous NaOH.

Generally all oxidation processes observed (except for processes of 0.55–0.58 V for Ni containing porphyrins which are due to oxidation of Ni(II) to Ni(III)) are due to oxidation of the porphyrin ring. The presence of Ni(III) in the films was confirmed by X-ray photoelectron spectroscopy. All of the compounds that were derivatives of the 3-methoxy-4-hydroxyporphyrin formed films by oxidative polymerization on the electrode surface and exhibited similar oxidative electrochemistry. Each undergoes oxidations at potentials 0.11–0.19 and 0.22–0.34 V for processes I and II, respectively. These potentials indicate that the first two oxidation processes occur relatively easily. This is rather unusual as porphyrins usually undergo two oxidations in the range of potentials 1.1–1.4 V. The mechanism of oxidation of 3-methoxy-4-hydroxyporphyrin leading to polymerization was published previously.[8] Two 3-methoxy-4-hydroxyphenyl substituents in the α and γ positions on the porphyrin ring are oxidized in two 2-e steps (peak I and II) to form highly reactive orthoquinone species adsorbed on the electrode surface. These species can oxidize a parent molecule and initiate the polymerization process. Polymerization of Zn(*p*-NH$_2$)TTPP occurs according to the mechanism proposed for polymerization of aniline.[13,14]

Figure 2 shows multiple scan cyclic voltammograms obtained during film formation with (a) Ni(1,10-phen)(TMHPP)$_2$, (b) Ni(*p*-NH$_2$)TMHPP, and (c) a 1:1 mixture of the two each having a total concentration of 5×10^{-5} M. Initially, the mixture shows a broad oxidation wave without discernible peaks over the range of potential in which processes I and II tend to be observed. This wave decreases and disappears in subsequent scans. This behavior and that of the other individual compounds are the same pattern observed for NiTMHPP itself as well as the

(20) Bettelzeim, A.; White, B. A.; Raybuck, S. A.; Murray, R. W. *Inorg. Chem.* 1987, *26*, 1009.

Table I. Anodic Peak Potentials Observed for Oxidation Process of TMHPP (in 0.1 M Aqueous NaOH) and TTPP (0.1 M TBAP in DMF; Potential Scan Rate 100 mV s^{-1})

compound	potential, V vs SCE			
	peak I	peak II	peak III	peak IV
H_2TMHPP[a]	0.12	0.32		
NiTMHPP[a]	0.14	0.34	0.58	
H_2(1,10-phen)(TTMHPP)$_2$	0.12	0.25		
Zn(1,10-phen)(TMHPP)$_2$	0.11	0.22		
Ni(1,10-phen)(TMHPP)$_2$	0.18	0.33	0.51	
H_2(1,10-phen)(TTPP)$_2$	0.21	0.31		1.08
Zn(1,10-phen)(TTPP)$_2$	0.75	0.85		1.20
Ni(*p*-pyr)TMHPP	0.19	0.24	0.50	
H_2(*p*-pyr)TTPP	0.83	0.94		1.10
Zn(*p*-NH_2)TMHPP	0.12	0.27	0.50	
Ni(*p*-NH_2)TMHPP	0.14	0.24	0.55	
Zn(*p*-NH_2)TTPP	0.78			1.21

[a] Taken from refs 6 and 8.

Table II. Wavelength of Maximum Absorption for UV-Visible Spectra of Monomeric Porphyrins in Aqueous or Dimethylformamide Solution

compound film	Soret	Q bands λ_{max}, nm		
H_2(1,10-phen)TMHPP)$_2$	430		604	686
Zn(1,10-phen)(TMHPP)$_2$	435		619	698
Ni(1,10-phen)(TMHPP)$_2$	430		544	
Ni(*p*-pyr)TMHPP	428		544	600
H_2(*p*-pyr)TTPP[a]	426	517	555	649
Zn(*p*-NH_2)TMHPP	437			622
Ni(*p*-NH_2)TMHPP	430		546	598
Zn(*p*-NH_2)TTPP[a]	425		560	601

[a] DMF solution.

other TMHPP species in this work—two oxidation peaks which decrease after the first scan.[8] All of the nickel species showed the internal monitor of film formation, the Ni(II)/Ni(III) couple (peak IIIa,c) that appears and increases. This couple also appears when the electrode is removed from substrate solution and put in a fresh solution of NaOH. This peak is observed at $E_{1/2}$ 0.45, 0.46, and 0.48 V for compounds a, b, and c, respectively (Figure 2).

Polymeric films can also be formed at constant potential electrolysis. Experimental results show that a 20–120-s deposition time at constant potential 0.7 V from solution concentrations about 5×10^{-5} M is sufficient to form stable, compact adherent films 10–15 equivalent monolayers thick and with a specific conductivity of 10–400 Ω^{-1} cm^{-1}. Electrodic properties of electrodes covered with these polymeric porphyrin films are better than those observed for an unmodified glassy carbon electrodes. Cyclic voltammograms obtained with all of the films studied show that peak separation of the $Fe(CN)_6^{3-}/Fe(CN)_6^{4-}$ couple is about 58 ± 2 mV, the value predicted for a reversible one-electron-transfer reaction. The $Fe(CN)_6^{3-}/Fe(CN)_6^{4-}$ couple was also used to estimate the electroactive surface area for the films studied.

Spectra obtained during oxidations of compounds that formed films showed a continuous decrease in adsorption with no new bands observed. These are typical observations for exhaustive electrolysis when the electrolysis products are not observable in solution. Typical spectra of unoxidized porphyrins exhibit Soret bands from 425 to 437 with several smaller Q bands in the range 500–750 nm (Table II). The thin-layer UV-visible spectra show a gradual decrease in all bands. No new bands characteristic of the products of oxidation of the porphyrin ring, the radical, and/or dication, appear.[21] Attempts at performing

(21) Chang, D.; Malinski, T.; Ulman, A.; Kadish, K. M. *Inorg. Chem.* 1984, *23*, 817 and references therein.

Table III. Wavelength and Maximum Absorbance of UV-Visible Spectra of Polymeric and Copolymeric Films Deposited on Indium Oxide Transparent Electrode

compound film	Soret	Q bands	
		λ_{max}, nm	abs
H_2(1,10-phen)(TMHPP)$_2$	447/0.20	582/0.15	881/0.15
Zn(1,0-phen)(TMHPP)$_2$	447/0.07	565/0.06	787/0.06
Ni(1,10-phen)(TMHPP)$_2$	438/0.15	546/0.06	735/0.02
Ni(*p*-pyr)TMHPP	442/0.19	548/0.04	
Zn(*p*-NH_2)TMHPP	445/0.32	577/0.10	618/0.28
Ni(*p*-NH_2)TMHPP	428/0.05	542/0.01	
Zn(*p*-NH_2)TTPP	423/0.20	519/0.10	690/0.20
Ni(1,10-phen)(TMHPP)$_2$ + Ni(*p*-pyr)TMHPP	428/0.014	531/0.004	
H_2(1,10-phen)(TMHPP)$_2$ + H_2(*p*-pyr)TTPP	426/0.045	519 sh 553sh	594 sh
Zn(1,10-phen)(TMHPP)$_2$ + Zn(*p*-NH_2)TTPP	430		
Ni(*p*-pyr)TMHPP + Zn(*p*-NH_2)TMHPP	438/0.17	538/0.02	567/0.01
Ni(1,10-phen)(TMHPP)$_2$ + Ni(*p*-NH_2)TMHPP	425/0.37	534/0.03	

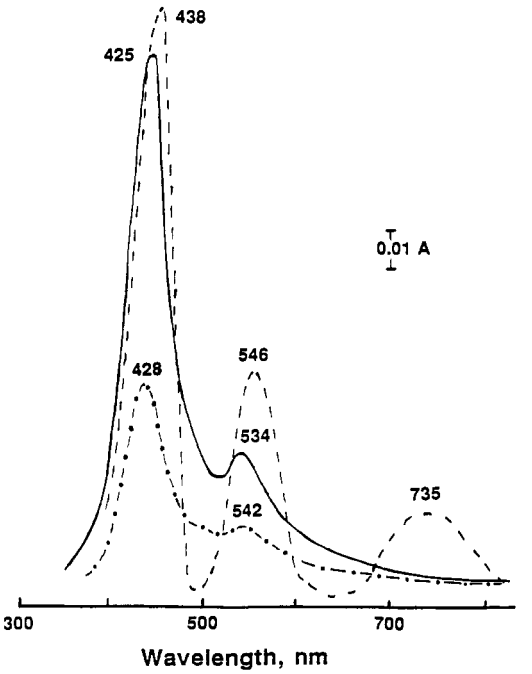

Figure 3. UV-visible absorption spectra of polymeric films of Ni(1,10-phen)(TMHPP)$_2$, (---); Ni(*p*-pyr)TMHPP (-·-) and copolymer of above two (—) deposited electrochemically on indium oxide transparent electrode at a constant potential of 0.6 V from 0.1 M NaOH.

spectroelectrochemistry during oxidative polymerization forming copolymers provided no new information as peaks were observed to decrease together. However, the fact that all peaks were observed to disappear indicate both monomeric species were removed from solution, e.g., utilized in the polymerization or copolymerization process.

Further evidence for the polymerization and copolymerization process is exhibited in the spectra observed for films formed on ITO electrodes. Table III summarizes spectral data obtained for all constituent compounds that formed films and the copolymer films formed. Figure 3 shows spectra obtained with (a) Ni(1,10-phen)(TMHPP)$_2$, (b) Ni(*p*-NH_2)TMHPP, and (c) a 1:1 mixture of the two. Comparison of the observed spectra lead to the following conclusion. The Soret peaks for polymeric Ni(1,10-phen)(TMHPP)$_2$ and Ni(*p*-NH_2)TMHPP are observed at 438 and 428 nm, respectively. The Soret peak for copolymer is observed at 425 nm. A low-absorption Q band

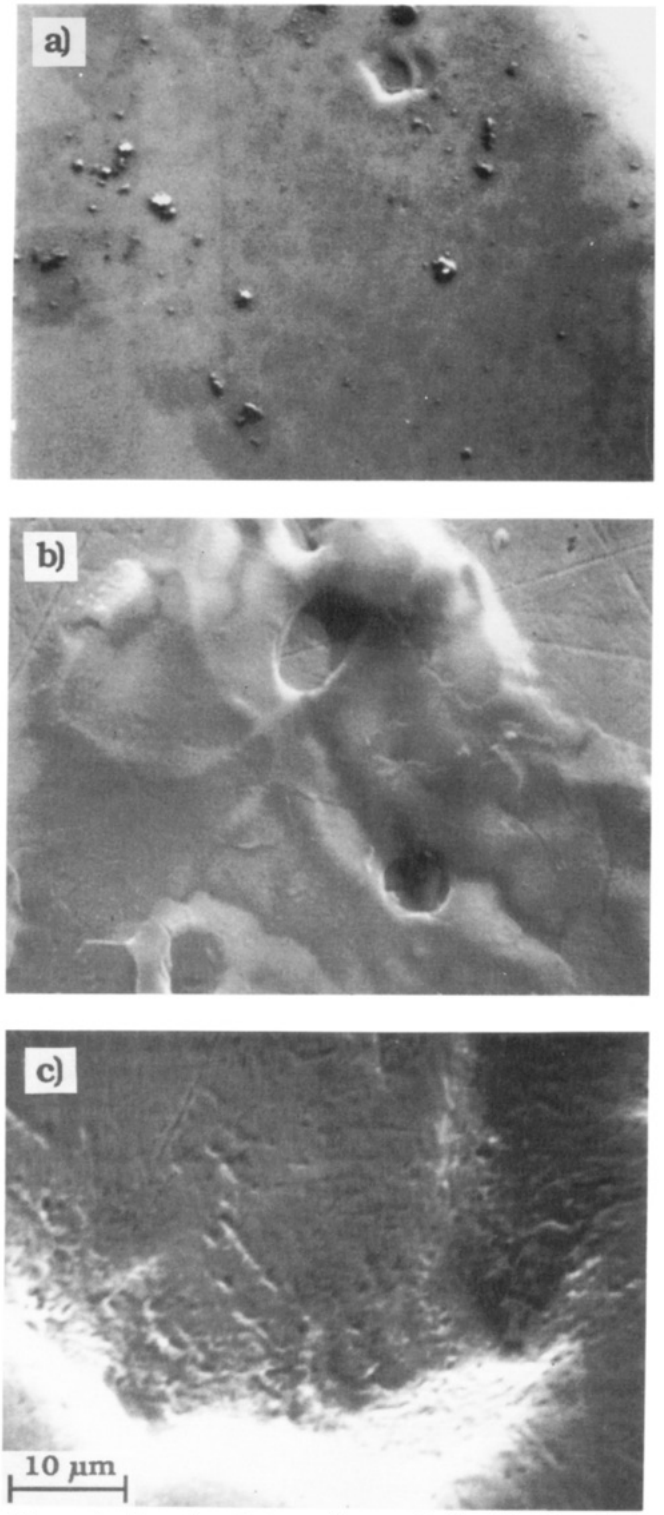

Figure 4. Scanning electron micrograph of a thin film of Ni(1,10-phen)(TMHPP)$_2$, (a), Ni(*p*-NH$_2$)TMHPP (b) and copolymer of above two (c) deposited electrochemically on Pt electrode at constant potential of 0.6 V from 0.1 M NaOH.

of copolymer at 525 nm is located also at the shorter wavelength in comparison to the low-absorption bands observed for polymeric films of Ni(1,10-phen)(TMHPP)$_2$ and Ni(*p*-NH$_2$)TMHPP at 546 and 542 nm, respectively. A band at 735 nm observed for polymeric Ni(1,10-phen)(TMHPP)$_2$ is not observed in the copolymeric film.

An experiment in which several monolayers of Ni(1,10-phen)(TMHPP)$_2$ was deposited on ITO followed by deposition of Ni(*p*-NH$_2$)TMHPP shows all peaks in a consistent position for each of the constituents. This is good

Table IV. Electrochemical Oxidation of Hydrazine on Polymeric and Copolymeric Porphyrins Electrodes in 0.1 M NaOH (Films Deposited at Constant Potential 0.7 V vs SCE on GCE)[a]

compound film	t_{dep}, s	ΔE_{pa}, mV
H$_2$(1,10-phen)(TMHPP)$_2$	60	0
	120	0
Zn(1,10-phen)(TMHPP)$_2$	60	0
	120	0
Ni(1,10-phen)(TMHPP)$_2$	60	0
	120	0
Ni(*p*-pyr)TMHPP	60	180
	120	220
Zn(*p*-NH$_2$)TMHPP	60	100
	120	320
Ni(*p*-NH$_2$)TMHPP	60	110
Zn(*p*-NH$_2$)TTPP	40	80
	60	160
Ni(1,10-phen)(TMHPP)$_2$ + Ni(*p*-pyr)TMHPP	60	120
Ni(1,10-phen)(TMHPP)$_2$ + Ni(*p*-NH$_2$)TMHPP	40	60
	60	110
Zn(1,10-phen)(TMHPP)$_2$ + Zn(*p*-NH$_2$)TTPP	20	330
	60	460
Ni(*p*-pyr)TMHPP + Zn(*p*-NH$_2$)TMHPP	60	180

[a] $\Delta E_{pa} = |E_{p_a}{}^c - E_{p_a}{}^p|$ where $E_{p_a}{}^c$ and $E_{p_a}{}^p$ are anodic potentials for oxidation of hydrazine on glassy carbon and porphyrin electrode, respectively.

evidence that the film deposited from the solution of Ni(1,10-phen)(TMHPP)$_2$ and Ni(*p*-NH$_2$)TMHPP is not a simple mixture of two polymeric materials but the copolymer. Scanning electron microscopy demonstrated that the films morphology is significantly different (Figure 4). A scanning electron micrograph (Figure 4a) of polymeric Ni(1,10-phen)(TMHPP)$_2$ grown electrochemically at a constant potential of 0.6 V on a platinum electrode for 5 min shows a smooth surface. The Ni(*p*-NH$_2$)TMHPP film obtained under similar conditions (Figure 4b) were rougher than the surface observed for Ni(1,10-phen)(TMHPP)$_2$. A scanning electron micrograph of a polymer of Ni(1,10-phen)(TMHPP)$_2$ and Ni(*p*-NH$_2$)TMHPP shows the morphology of the film to be relatively smooth with no microspheroid features visible with a magnification of 1890:1 (Figure 4c). An electrochemically active area (measured based on Fe^{2+}/Fe^{3+} redox reaction) which reflects a roughness of the film compared to the active area of platinum electrode was 1.01, 1.12, and 1.05 for polymeric Ni(1,10-phen)(TMHPP)$_2$, Ni(*p*-NH$_2$)TMHPP and copolymer, respectively. This again confirms the smooth surface of the films.

Another evidence for the existence of copolymer films as actual new materials can be found in the data obtained from catalytic studies. Substrates used for catalytic studies are hydrazine, methanol, and dioxygen in acid and base. Catalytic effects observed with copolymer films include significant enhancement, averaging and no enhancement as compared to the films formed by polymerization of constituents alone.

Oxidation of Hydrazine. Previous results had shown poly-NiTMHPP to act as a good electrocatalyst for the oxidation of hydrazine.[8] Catalytic activity was evaluated by determining the shift of oxidation potential in the negative direction and current increase for the polymer covered versus the bare GCE. As with poly-NiTMHPP, the oxidation product was N_2. Results, including deposition time to achieve maximum catalytic effect, are shown in Table IV.

The (1,10-phen)(TMHPP)$_2$ polymers show no catalytic effect. However, the amino- and pyrrole-substituted TMHPP polymers exhibit a catalytic effect, with the

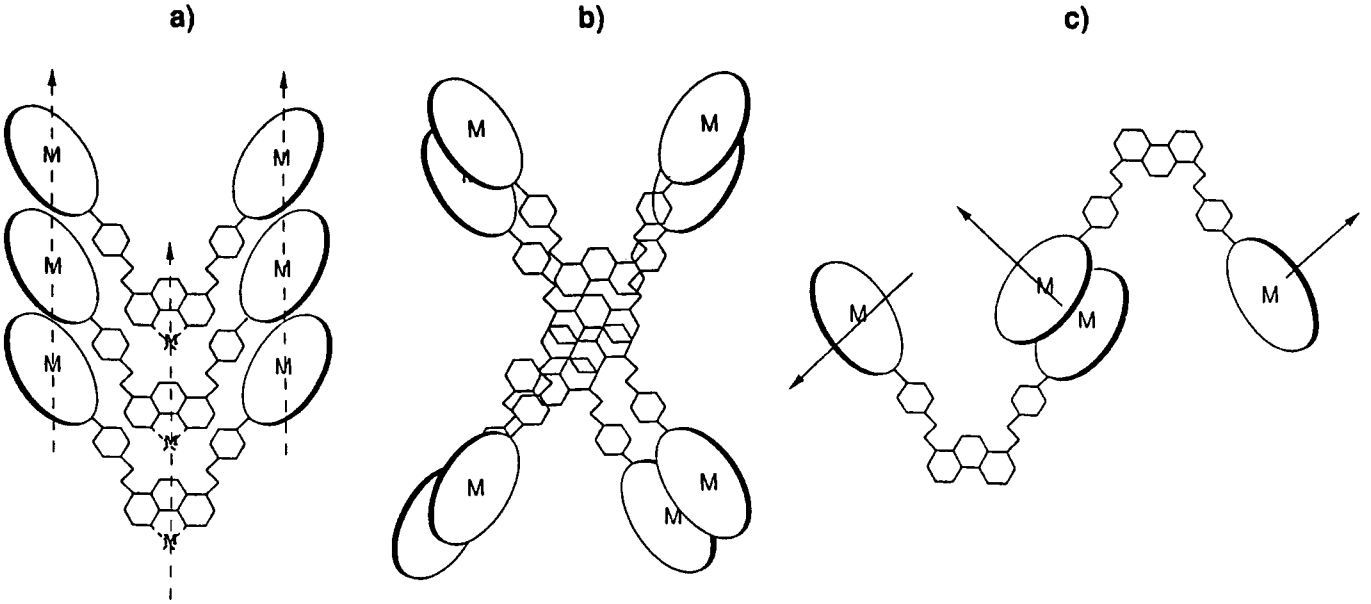

Figure 5. Possible spatial arrangements of free base and metalated (1,10-phen)(TMHPP)$_2$ in polymeric films: (a) in the case of (1,10-phen)(TMHPP)$_2$ metalated at the phenanthroline spacer N(1)N(10) centers in both porphrin rings; (b) as in (a) with different spatial arrangement; (c) another 3-D variant.

highest obtained with polymeric films containing zinc as the central metal. The copolymers formed from amino- and pyrrole-substituted TMHPP show an "averaging" effect—not as good as the amino and pyrrole substrate alone but increased over the 1,10-phenanthroline diporphine. These observations can be explained based on a concentration effect. The presence of the inactive 1,10-phenanthroline diporphine in the film dilutes the amino and pyrrole species.

Copolymers of the free base of the TMHPP series with the tolyl series, TTPP, show enhanced catalysis over their constituents. The potential shift is 190 mV. Again the (1,10-phen)(TMHPP)$_2$ shows no catalytic effect and the (*p*-pyr)TTPP does not form a film to exhibit catalysis. In this case, it may be that the catalytic effect is independent of the presence of the 3-methoxy-4-hydroxy moieties, because it is centered in the porphyrin. The function of the 1,10-phenanthroline diporphine is to promote the film formation.

A significant enhancement in catalysis is observed with the copolymer formed from the Zn(1,10-phen)(TMHPP)$_2$ and the Zn(*p*-NH$_2$)TTPP. The shift in peak potential, 460 mV, is almost 3 times as high as that observed for Zn(*p*-NH$_2$)TTPP, which forms films on its own. The explanation for enhancement would seem to be due to a structural effect or the spatial arrangement promoted by the 1,10-phenanthroline diporphine. The catalytic effect observed with the copolymer formed from Ni(*p*-pyr)TMHPP and the Zn(*p*-NH$_2$)TMHPP, 180 mV, was worse that either of the constituents, 320 and 220 mV, respectively.

Figure 5 shows types of stacking promoted by the phenanthroline linkage as in H$_2$(1,10-phen)(TMHPP)$_2$ particularly after metalation at the phenanthroline N(1)N(10) centers. Also, interactions between two porphyrin rings located fairly close together in the same molecule would be expected (Figure 5c). Because the 3-methoxy-4-hydroxyphenyl substituents are both polar and could be involved in hydrogen bonding within the stacked films intermolecular attractions probably also occur.

Oxidation of Methanol. Previous results had shown poly-NiTMHPP to be a good electrocatalyst for the oxidation of methanol in basic solution.[8] As with poly-NiTMHPP, the oxidation product was CO_2. Results are shown in Table V. The current density observed was 3–5 times higher than that observed for oxidation of methanol on bare platinum electrode.

Table V. Electrooxidation of Methanol on Polymeric and Copolymeric Porphyrin Electrodes in 0.1 M NaOH (Films Deposited at Constant Potential 0.7 V vs SCE on Platinum Electrode)

compound film	t_{dep}, s	ΔE_{pa}, mV
H$_2$(1,10-phen)(TMHPP)$_2$	20	80
	120	100
Zn(1,10-phen)(TMHPP)$_2$	20	80
	120	110
Ni(1,10-phen)(TMHPP)$_2$	20	70
	120	100
Ni(*p*-pyr)TMHPP	20	110
	120	120
Ni(*p*-NH$_2$)TMHPP	20	90
	60	100
Zn(*p*-NH$_2$)TTPP	20	90
	60	110
Ni(1,10-phen)(TMHPP)$_2$ + Ni(*p*-pyr)TMHPP	20	110
	60	140
Ni(1,10-phen)(TMHPP)$_2$ + Ni(*p*-NH$_2$)TMHPP	20	100
	60	120
Zn(1,10-phen)(TMHPP)$_2$ + Zn(*p*-NH$_2$)TTPP	20	110
	60	120
Ni(*p*-pyr)TMHP + Zn(*p*-NH$_2$)TMHPP	20	90
	120	110

[a] $\Delta E_{p_a} = |E_{p_a}{}^c - E_{p_a}{}^p|$ where $E_{p_a}{}^c$ and $E_{p_a}{}^p$ are anodic potentials for oxidation of methanol on glassy carbon and porphyrin electrode, respectively.

The (1,10-phen)(TMHPP)$_2$ polymeric film shows some catalytic effect for the oxidation of methanol. The effect with the nickel species is the least and is maximized for thin films. The free-base and zinc species give greater negative shifts in oxidation potential (ΔE_{pa} = 20 mV) for deposition times up to 120 s. The effect shown by the Ni(*p*-pyr)TMHPP is the highest observed among the polymeric materials studied. The effect of Ni(*p*-pyr)-TMHPP is slightly less than the corresponding pyrrole and maximizes at the same film deposition time. The pyrrole zinc species were not investigated in these studies. The catalysis on Zn(*p*-NH$_2$)TPP is about as good as that achieved for any of the previous species, ΔE_{pa}, 110 mV.

Maximum catalysis for this film is achieved at t_{dep} = 60 s, and the effect decreases with longer deposition times.

None of the copolymers show an "averaging" effect for the catalysis of methanol. In this case, a dilution/concentration effect would not be expected because the 1,10-phenanthroline diporphines as well as the amino and pyrrole species act as catalysts. Copolymer deposition times were chosen so that films were deposited in the range of times in which the substituents exhibited maximum activity. Thus, short deposition times were chosen based on the smaller constituents rather than the long times required by the 1,10-phenanthrolines to exhibit maximum activity.

Copolymers formed from porphyrins with the pyrrole or amino substituent with the 1,10-phenanthroline diporphine demonstrates a slight 10–20-mV potential shift for methanol oxidation. Copolymers of the free base of the TMHPP series with the tolyl series, TTPP, show enhanced catalysis over their constituents. The ΔE_{pa} is −110 mV for a 20-s deposition time. This is 30 mV greater than that observed for the 1,10-phenanthroline diporphine at comparable times and still greater than the maximum exhibited by this species. The (*p*-pyr)TTPP alone does not form a film to exhibit catalysis.

The enhancement in catalysis observed with the copolymer formed from the Zn(1,10-phen)(TMHPP)$_2$ and the Zn(*p*-NH$_2$) TTPP is not as significant as that observed for the catalysis of hydrazine. The shift in peak potential is only 10 mV greater than that observed for Zn(*p*-NH$_2$) TTPP films, but it is 40 mV greater than the Zn(1,10-phen)(TMHPP)$_2$ at comparable deposition times. This would again be a case where the explanation for enhancement lies in a structural effect or spatial arrangement promoted by the 1,10-phenanthroline diporphine.

The catalytic effect observed with the copolymer formed from Ni(*p*-pyr)TMHPP and the Zn(*p*-NH$_2$)TMHPP was about the same as the more active constituent for short deposition times and slightly better for longer depositions. This is different than the effect on hydrazine catalysis which was not as good as either of the constituents and, again, the explanation probably lies in an effect of structure or spatial arrangement. A maximum current density (1.1 mA/cm^2) for methanol oxidation obtained on Ni(1,10-phen)(TMHPP)$_2$ + Ni(*p*-pyr)TMHPP electrode is 7 times higher than that observed on the platinum electrode (0.16 mA/cm^2). Platinum is considered to be one of the best catalysts for methanol oxidation.[22] The current density higher than 0.80 mA/cm^2 (5 times higher than on platinum) was obtained for methanol oxidation on other polymeric and copolymeric films studied in this work.

Reduction of Oxygen. Optimal catalytic reduction of dioxygen directly to water is indicated by a value of 3.2 μA/[(V/s)$^{1/2}$ cm^2] for the slope of the voltammetric peak of the four-electron reduction of oxygen.[20] Previous results had indicated that poly-NiTMHPP would not be a good electrocatalyst for the reduction of oxygen directly to water in basic solution because production of a small amount of hydrogen peroxide was observed.[7,8] In the present studies, results obtained in basic solution are not promising. There were negligible shifts in peak potentials, and the slopes were less than 0.8 μA/[(V/s$^{1/2}$) cm^2]. These data are not presented. Table VI summarizes the data obtained for the electroreduction of dioxygen in acid solution (0.5 M H_2SO_4). All of the films studied, including the (1,10-phen)(TMHPP)$_2$, show a catalytic effect for the reduction of dioxygen. The slopes obtained for polymeric films are all less than the optimal value. However, all of the copolymers except Ni(*p*-pyr)TMHPP + Zn(*p*-NH$_2$)TMHPP give a slope equal to the optimal value, 3.2 μA/[(V/s$^{1/2}$) cm^2].

Table VI. Electroreduction of Dioxygen on Polymeric and Copolymeric Porphyrins in 0.1 M H_2SO_4 (Films Deposited at Constant Potential 0.6 V vs SCE on Platinum Electrode for 40 s)[a]

compound film	ΔE_{pc}, mV	slope, μA/[(V/s)$^{1/2}$ cm^2]
H_2(1,10-phen)(TMHPP)$_2$	0.13	3.07
Zn(1,10-phen)(TMHPP)$_2$	0.14	2.61
Ni(1,10-phen)(TMHPP)$_2$	0.13	2.64
Ni(*p*-pyr)TMHPP	0.16	2.59
Zn(*p*-NH$_2$)TMHPP	0.17	3.09
Ni(P-NH$_2$)TMHPP	0.14	2.72
Zn(*p*-NH$_2$)TTPP	0.16	3.07
Ni(1,10-phen)(TMHPP)$_2$ + Ni(*p*-pyr)TMHPP	0.13	3.20
H_2(1,10-phen)(TMHPP)$_2$ + H_2(*p*-pyr)TTPP	0.14	3.20
Ni(1,10-phen)(TMHPP)$_2$ + Ni(*p*-NH$_2$)TMHPP	0.13	3.20
Zn(1,10-phen)(TMHPP)$_2$ + Zn(*p*-NH$_2$)TTPP	0.13	3.20
Ni(*p*-pyr)TMHPP + Zn(*p*-NH$_2$)TMHPP	0.13	3.15

[a] $\Delta E_{pc} = |E_{pc}^{c} - E_{pc}^{p}|$ where E_{pc}^{c} and E_{pa}^{p} are cathodic potentials for reduction of oxygen on platinum and porphyrin electrode, respectively.

A small second peak at potential about 0.75 V due to reduction of hydrogen peroxide to water, was observed for all polymeric materials studied and also for copolymeric Ni(*p*-pyr)TMHPP + Zn(*p*-NH$_2$)TMHPP. It is interesting to note that all of the copolymers with a slope equal to the theoretical value show only one oxygen reduction wave. Voltammetric measurements with a rotating ring-disk electrode (platinum disk covered with copolymeric film and platinum ring) indicate no detectable amount of hydrogen peroxide was generated in the process of oxygen reduction on electrodes covered with copolymers that had the optimal slope.

The unexpected result, is the excellent catalytic effect observed on the copolymeric materials with no central metal coordinated to the porphyrin: H_2(1,10-phen)(TMHPP)$_2$ + H_2(*p*-pyr)TTPP. It has been assumed—based on previous studies of catalytic electron reduction of oxygen on porphyrins or phthalocyanines—that the catalysis occurs only on metalated materials. The best results for electrocatalytic reduction of oxygen has always been observed for porphyrins or phthalocyanines with cobalt as a central metal. This has led to the hypothesis that efficient catalysis is possible only for systems where oxygen or hydrogen peroxide are immobilized by axial ligation on the metal center.

Metalated porphyrins may undergo demetalation in acidic media. Loss of metal will be followed by significant decrease of catalytic effect. The demetalation process seriously limits the application of metalloporphyrins as catalysts for fuel cells. The high catalytic effect observed in this work for copolymer obtained from porphyrinic free bases require further studies but indicates potential application of this new material in fuel cells.

Conclusion

These studies present evidence to show that several novel porphyrins undergo oxidative polymerization and copolymerization leading to formation of conductive films on glassy carbon and platinum electrodes. The new copolymeric materials can have significantly altered elec-

(22) Cameron, D. S.; Hards, G. A.; Harrison, B.; Potter R. J. *Platinum Met. Rev.* 1987, *31*, 177.

trocatalytic properties of electrodes Copolymers of Zn(1,10-phen)(TMHPP)$_2$ and Zn(*p*-NH$_2$)TTPP show significant enhancement of catalytic process over their constituents. This is especially true for electrocatalytic oxidation of hydrazine and reduction of oxygen directly to water. Generally, electrocatalytic reduction of oxygen is enhanced for all copolymers studied. One of the other important conclusion of these studies is the fact that porphyrinic polymeric and copolymeric materials show high catalytic activity in oxygen reduction even in the absence of coordinated metal.

Registry No. H$_2$(*p*-NH$_2$), 141509-35-5; H$_2$(*p*-NHAc), 141509-34-4; Zn(*p*-NH$_2$)(TMHPP), 141526-70-7; H$_2$(1,10-phen)(TMHPP)$_2$, 141509-36-6; H$_2$(*p*-pyr)TMHPP, 141509-37-7; Ni(*p*-pyr)TMHPP, 141526-71-8; H$_2$(*p*-pyr)TTPP, 141509-38-8; NI[H$_2$(*p*-pyr)]TTPP, 141526-72-9; H$_2$(1,10-phen)(TMHPP)$_2$ (homopolymer), 141526-68-3; Ni(*p*-pyr)TMHPP (homopolymer), 141526-73-0; Zn(*p*-NH$_2$)TMHPP (homopolymer), 141526-74-1; Ni(*p*-NH$_2$)TMHPP (homopolymer), 141526-76-3; Zn(*p*-NH$_2$)-TTPP (homopolymer), 133091-18-6; H$_2$(1,10-phen)(TMHPP)$_2$/H$_2$(*p*-pyr)TTPP (copolymer), 141526-69-4; Ni(*p*-pyr)TMHPP/Zn(*p*-NH$_2$)TMHPP (copolymer), 141526-77-4; AcNHC$_6$H$_4$-*p*-CHO, 122-85-0; H$_2$NNH$_2$, 302-01-2; CH$_3$OH, 67-56-1; O$_2$, 7782-44-7; H$_2$O, 7732-18-5; pyrrole, 109-97-7; 1,1-phenanthroline-4,7-dicarbonyl chloride, 130897-90-4; 2,5-diethoxytetrahydrofuran, 3320-90-9; *meso*-tri-*p*-tolyl(*p*-aminophenyl)porphyrin, 73170-32-8.

Photoresists on the Base of the Poly(hydroxyamines) and Poly(hydroxyamino esters)

A. Yu. Kryukov and A. V. Vannikov*

A. N. Frumkin Institute of Electrochemistry, Russian Academy of Sciences, Leninsky Prospect, 31, 117071 Moscow, Russia

A. V. Anikeev and L. I. Kostenko

Institute of Physico-Organic Chemistry and Coal Chemistry, Ukrainian Academy of Sciences, R. Luxemburg, 70, 340114 Donezk, Ukraine

Received December 6, 1991. Revised Manuscript Received February 24, 1992

The linear poly(hydroxyamines) (PHA) and poly(hydroxyamino esters (PHAE) of various structures have been synthesized. PHA and PHAE exhibit peculiar photochemical and physicochemical properties which make them suitable for producing new high-sensitivity photoresists. The influence of chemical structure and molecular weight of the polymers on the photochemical characteristics and on the development kinetics of photoresists based on PHA and PHAE has been investigated.

Introduction

Linear poly(hydroxyamino ethers) (PHAE) synthesized by step growth addition reactions of secondary diamines or primary monoamines to bisphenol diglycidyl ethers [1-3] are under intensive investigation due to the opportunity of application in electrophotography.[4-6] In the presence of halogen-containing acceptors, for example, CBr$_4$, PHAE are oxidized under the action of light. The mechanism of photochemical transformation, in which a charge-transfer complex (CTC) plays the main role, was studied in detail in papers[7,8] The CTC is formed between the acceptor and an electron-donor amino group in polymer chain. The main product of photooxidation in such systems is a polycation with the structure dependent on the structure of the amine fragment. With the transition from nonpolar polymer to ionic polymeric photoproduct, the solubility changes resulting in selective dissolution between exposed and unexposed area making the films based on PHAE useful as photoresists.[9-11] It is important to note that the regarded systems possess some advantages in comparison with the known resists based on CBr$_4$[12-14] as the former ones have higher sensitivity due to the optical amplification. The optical amplification of the latent image is realized by the flood irradiation of the exposed sample with red and near IR light, $\lambda \geq 650$ nm. The light is absorbed only by the polycations (the latent image centers) that acts as an autosensitizer.

Many monoamines as well as diamines were used for the synthesis of PHAE described in the recent works.[1,2,15,16]

(1) Horhold, H.-H.; Klee, J.; Bellstedt, K. *Z. Chem.* **1982**, *22*, 166.
(2) Klee, J.; Horhold, H.-H.; Tonzer, W.; Fedtke, M. *Angew. Makromol. Chem.* **1987**, *147*, 71.
(3) Stolle, Th.; Pietsch, H.; Ebert, I. *Acta Polym.* **1987**, *38*, 340.
(4) Opferman, J.; Horhold, H.-H.; Markiewitz, N.; Pietsch, H. *J. Inf. Rec. Mater.* **1987**, *15*, 277.
(5) Vannikov, A. V.; Kryukov, A. Yu. *J. Inf. Rec. Mater.* **1990**, *18*, 345.
(6) Markiewitz, N.; Pietsch, H.; Bilke, W.-D.; Post, M.; Wannikow, A. W.; Kryukow, A. Ju. *Acta Polym.* **1987**, *38*, 347.
(7) Kryukov, A. Yu.; Vannikov, A. V.; Markiewitz, N. N.; Post, M. Zh. *Nauchn. Prikl. Photogr. Kinematogr.* **1989**, *34*, 361.
(8) Tkachev, V. A.; Malt'zev, E. I.; Vannikov, A. V.; Kryukov, A. Yu. *Res. Chem. Intermed.* **1990**, *137*, 7.
(9) Kryukov, A. Yu.; Tkachev, V. A.; Vannikov, A. V.; Markiewitz, N. N.; Post, M.; Horhold, H.-H. *Vysokomolek. Soed.* **1990**, *32* (B), 548.
(10) Kryukow, A. Yu.; Post, M.; Wannikow, A.; Markiewitz, N.; Pietsch, H.; Horhold, H.-H. GDR Patent 250388, 1987.
(11) Markiewitz, N.; Post, M.; Abraham, H. W.; Mheliss, G.; Rabe, C.; Horhold, H.-H.; Kryukow, A.; Wannikow, A. W.; Tkachew, W. GDR Patent 277537, 1990.
(12) Moreau, M. *Semiconductor Lithography*; Plenum Press: New York, 1988; Chapter 5.
(13) Hiraoka, H.; Chiong, K. N. *J. Vac. Sci. Technol. B* **1987**, *5*, 386.
(14) Vannikov, A. V.; Grishina, A. D. *Polym. Sci. USSR* **1990**, *32*, 1725.
(15) Klee, J.; Horhold, H.-H.; Tonzer, W.; Fedtke, M. *Acta Polym.* **1986**, *37*, 272.

0897-4756/92/2804-0803$03.00/0